Microstructural influence on fatigue crack growth

Michael Marx[1,a], Wolfgang Schaef[1,b], Tao Qian[1,c]

[1] Insitute of Materials Science and Methods, Saarland University,
Campus D2 2, 66123 Saarbruecken, Germany

[a] m.marx@matsci.uni-sb.de, [b] w.schaef@saarschmiede.com, [c] t.qian@matsci.uni-sb.de

Keywords: fatigue, short cracks, FIB-tomography, UFG materials

Abstract
Fatigue induced fracture is the number one reason for failure of technical systems. Thereby there are a lot of approaches to strengthen a material against fatigue cracks for instance by using the strengthening effect of grain boundaries. Especially in the stage of short crack growth it is well known that grain boundaries lead to a fluctuating crack propagation rate with a deceleration of the crack growth rate in front of the grain boundaries sometimes combined with a complete stop for a large number of cycles. We identified some of the interaction mechanisms which are responsible for this behaviour by focused ion beam (FIB) artificial crack initiation combined with in-situ fatigue testing in the scanning electron microscope and FIB tomography. The results include useful aspects for fatigue life calculation and to make materials fatigue resistant.

Introduction
Materials and components exposed to cyclic loading spent up to 90 % of their lifetime by the growth of short cracks which nucleate and grow crystallographically on single slip planes and interact with grain boundaries, phase boundaries or precipitates [1, 2, 3]. Thereby the dislocations emitted at the crack tip are blocked at boundaries or have to pass precipitates by an Orowan process. Consequently short cracks are strongly influenced by the local microstructure which leads to the typical fluctuating crack growth not described by continuum models [4-9]. However, for a correct life time prediction the interaction of cracks with microstructural barriers must be understood. Furthermore a fundamental understanding can help making materials fatigue resistant. A theoretical description of the interaction can be found in the original BCS model and the modified form of Tanaka [5], Navarro, de Los Rios [6] and Zhai [10, 11] which are also described in [12]. There are several simulations so far investigating different influences of microstructural barriers against short crack propagation [13, 14]; however, there is a lack in experimental work due to the complexity when excluding as many parameters as possible which can influence the crack propagation additionally to the barriers. And it is not clear which parameters have to be included in the simulations to map reality as good as possible. For instance if one is interested in the fatigue resistance of special grain boundaries like different sigma boundaries, one has to keep the crack parameters crack length, geometry, distance to the grain boundary and driving force constant. This is not possible for natural cracks. Therefore we developed and established a method for artificial crack initiation by focused ion beam (FIB) to perform systematic experiments on the interaction between short fatigue cracks and the microstructural obstacles in metallic materials [15, 16]. The basic idea is to cut micro-

notches directly on the slip plane with the highest Schmid factor by the FIB as initiation sites for stage I fatigue cracks after measuring the crystallographic orientation of the initial grain by electron backscatter diffraction (EBSD). The advantage of this method is that firstly the position of the micro-notch can be chosen before the experiment in respect to a selected microstructural barrier, e.g. a special grain boundary identified by EBSD. This can be done with an accuracy of about 1 µm. Secondly it is possible to define the initial crack length and depth to exclude these parameters as variables.
Further information can be obtained by FIB-tomography which enables the 3D-reconstruction of sub-surface crack paths and the surrounding microstructural features with high spatial resolution. Introducing this method was a first step to quantify common theoretical models for short fatigue crack growth based on dislocation pile up at grain boundaries [5, 6] and on geometrical aspects of the microstructural obstacles [10, 11]. By measuring the crack propagation near microstructural obstacles in coarse grained nickel based superalloy several important results about the mechanisms of interaction were obtained. In the second step different crack and grain boundary parameters were varied. This is very important to verify the results of simulations to get a complete understanding of the interaction mechanisms and thereby ideas to produce fatigue resistant materials.

Experimental

So far we investigated different materials and microstructures: As mentioned above a nickel based superalloy was used to investigate the physical mechanisms of crack propagation and the interaction of cracks with grain boundaries according to the BCS model in the modified form of Tanaka, Navarro, de Los Rios and Zhai. Therefore the single crystalline nickel based superalloy CMSX-4 was used in a polycrystalline modification which was solidified in a Bridgman vacuum investment casting unit. The chemical composition is shown in table 1, for further details see [12]. As result a polycrystalline version of CMSX-4 with grain sizes in the order of several millimetres could be obtained (CG-CMSX4). The γ´-precipitates were small (300 nm) compared to the crack size (50 µm and more) used in our experiments and did not show any influence on the scale where the crack propagation was investigated.
As technical high strength material widely used in the airplane industry the aluminium alloy 7075-T7 was used, the chemical composition is shown in table 2. The heat treatment was performed according to [17]. As result there was a thermodynamically stable microstructure with a fine distribution of $MgZn_2$ intermetallic precipitates.
As second construction material widely used mild steel was investigated. The chemical composition of the mild steel is given in table 3. The steel sheets were solution treated at 1200 °C for 8 hours under vacuum to increase the grain size up to approximately 200 µm and afterwards heated at 710 °C on air for two hours with subsequent water quenching. The heat treatment was followed by an aging for 4 weeks at room temperature to suppress the formation of cyclic Lüders bands during fatigue testing.

Table 1: Chemical composition of CMSX4 after recasting, measured by EDX (weight-%)

	Al	Ti	Co	Mo	Ta	W	Re	Cr	Ni
wt.%	5,4	0,8	10,5	1,1	2,1	10,5	6	6,9	balance

Table 2: Chemical composition of the Al 7075-T7, measured by EDX (weight-%)

	Zn	Mg	Cu	Fe	Si	Mn	Cr	Ti	Al
wt.%	5,1-6,1	2,1-2,9	1,2-2,0	0,5	0,4	0,3	0,2-0,3	0,2	balance

Table 3: Chemical composition of the mild steel, measured by spark spectroscopy (weight-%)

	C	Si	Mn	P	S	Mo	Ni	Al	Cu	Fe
wt.%	0.1	0.17	0.55	0,006	0,019	0,04	0,12	0,007	0,19	balance

Finally as a modern high strength material, bimodal ultra-fine grained (UFG) nickel was investigated. The bimodal microstructure was produced by a heat treatment of nanocrystalline (NC) nickel synthesized by pulsed electro deposition (PED). The tensile specimens were then annealed at 500°C in vacuum for different durations to form bimodal microstructures. The result was a microstructure consisting of single UFG grains in the order between 500 nm and 1µm in a NC matrix with grain sizes less than 100 nm.

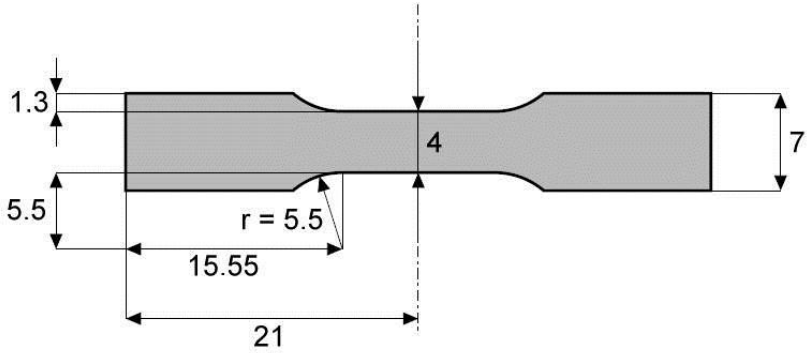

Fig. 1: Geometry of the fatigue specimens, the thickness varied between 1 mm and 2.5 mm

From all materials flat fatigue specimens comparable to figure 1 were cut by electrical discharge machining and afterwards mechanically grinded and polished followed by electro polishing to reveal an appropriate surface quality for EBSD measurements. By the EBSD measurements the mean grain size was measured and the orientations of the surface grains were revealed to calculate the optimum alignment of the micro-notches for the initiation of the artificial plane stage I cracks. This was done by calculating the slip plane with the highest Schmid factor for all fcc materials and by calculating the pencil glide plane according to Taylor [18] for the bcc steel [19]. The micro-notches were cut using the FIB, the alignment of the notches was reached by twisting and tilting the sample in respect to the ion beam. The acceleration voltage of the beam was 30 kV with a beam current of 20 nA. The notches were lens shaped to reach a semi penny-shaped profile in depth due to the limited aspect ratio of the ion milling technique, details can be found in [15].
For CG-CMSX4 special grain boundaries were selected as described in the results. Additionally the influence of the distance between crack and grain boundary was investigated for different grain boundaries. For each grain boundary two cracks were initiated at a distance of 30 µm and 50 µm respectively in front of the boundary. For Al 7075-T7 several cracks were initiated 10 µm in front of randomly selected high angle boundaries. Altogether five steel samples have been tested with three to five notches per sample. A distance of at least 5 grains between these notches was achieved to suppress mutual influences. Each notch was placed quite in the middle of the biggest grains with a distance of approximately 80 µm to the grain boundaries at both sides. For UFG nickel several cracks with an initial crack length of 100 µm were cut in the middle of the samples perpendicular to the loading axis. In this case the cracks were much longer than the largest grains, therefore a stage I crack initiation and propagation was not expected.
The fatigue tests were carried using a servo hydraulic testing machine with a sinusoidal load profile. The amplitude, frequency and load ratio varied with the tested materials as it can be seen in table 4. Fatigue crack growth was monitored via replica imaging and subsequent crack length measurement

on the replicas in a scanning electron microscope (SEM) for all samples. Some samples were selected for in-situ testing in the SEM for several hundred cycles and to measure the CTOD under load. Other samples were selected for a 3D FIB-tomography by the slice and view technique as described in [16].

Table 4: Parameters of the fatigue tests

material	load amplitude	Frequency	R-ratio	Initial crack length	in-situ	tomography
CG-CMSX4	300 MPa	5 Hz	- 0,1	100 µm	-	√
mild steel	300 MPa	5 Hz	-0,1	40 µm	-	√
Al 7075-T7	230 MPa	2 Hz	-1	30 µm	√	-
UFG nickel	350 MPa	2 Hz	-1	100 µm	√	-

Results and discussion

Crack growth in CG-CMSX4: Interaction mechanism between cracks and grain boundaries: Crack propagation through a boundary is a three dimensional problem. Therefore, FIB tomography was performed to get the information about the crack path in relation to the grain boundary and the involved slip planes in three dimensions. Here the results are shown for a special boundary where the crack passed the boundary in a straight way (Fig. 2a) but on a microscopic scale this was not the case. As it can be seen in figure 2b, the crack propagated on two slip planes and produces steps to pass the boundary.

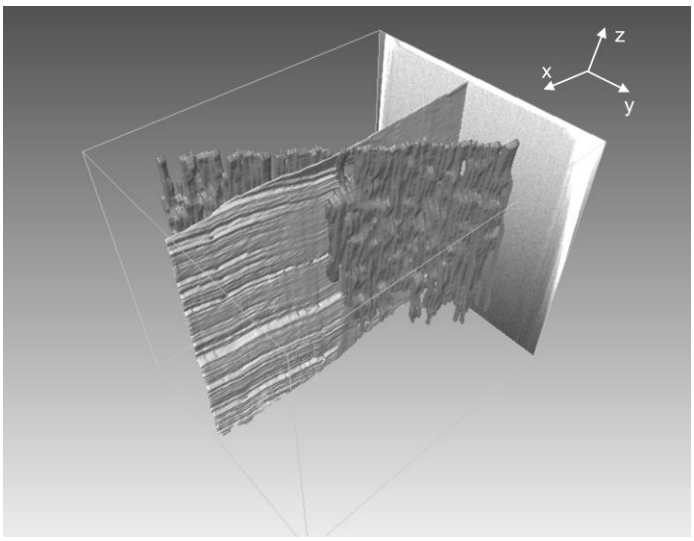

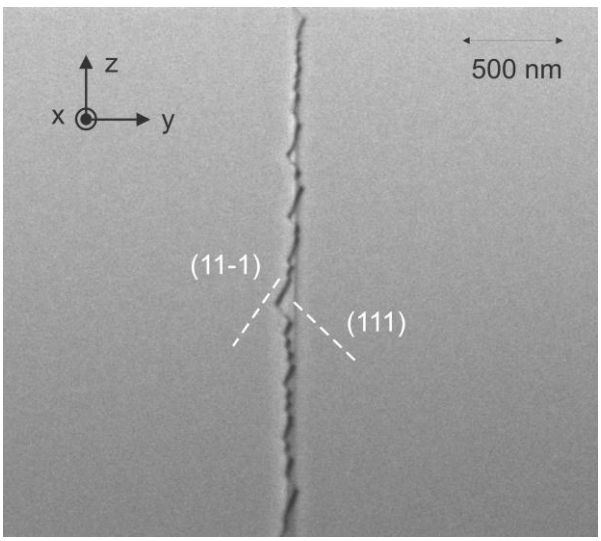

Fig. 2a: Wavy crack path after passing the grain boundary while the crack is straight on the surface

Fig. 2b: The steps on the crack plane produced by alternating activation of two slip planes

This crack stopped completely in front of the boundary for 2000 cycles while another crack only decreased the propagation rate as shown [12]. From the EBSD measurements the orientation of the possible slip systems and the position of the grain boundaries could be revealed as follows: For both grain boundaries all (111) planes of the adjacent grain had large misorientation angles in relation to the (111) plane of the grain where the cracks were initiated. This means that all possible (111) slip planes of the neighboring grains were not compatible. Therefore the influence of the grain boundary was expected to be the same. The difference between the two cracks was that in one case the

intersecting line between the initiating slip plane and one of the possible slip planes in the adjacent grain laid on the grain boundary. In the other case, there was no intersecting line between the initial slip plane and any of the possible slip planes in the second grain compatible with the grain boundary. Therefore due to the model of Zhai, the grain boundary must be ripped off which needs additional energy to create free surface. To avoid the ripping off the nano-steps were produced as shown in figure 2b. Details can be found in [12]

Fatigue crack growth in CG-CMSX4: Influence of the initial distance between crack and grain boundary. To measure the influence of the crack parameters crack length and distance between crack tip and grain boundary on the interaction strength, different cracks interacting with the same grain boundary in CG-CMSX4 were used. By the FIB crack initiation the crack parameters were varied while keeping the grain boundary constant. The results (Fig. 3) show a strong deceleration of the crack that initiated closer to the boundary (30 µm) while for the other cracks (50 µm) only a little deceleration can be seen. For the nearer notches crack growth could only be observed until the grain boundary was reached. Then the crack arrested over a period of several thousand cycles at the grain boundary until crack growth could be observed again and it took further some thousand cycles until the crack overcame the grain boundary. In contrast, no crack arrest was observed for the notch with the greater distance to the boundary. After the "slow crack" passed the grain boundary at a total length of approximately 90 µm, both cracks showed the same velocity.

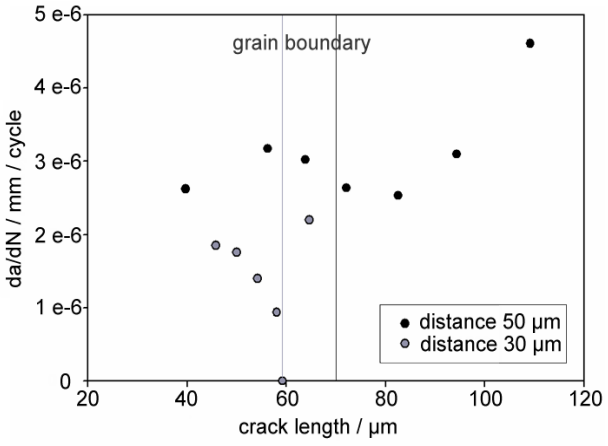

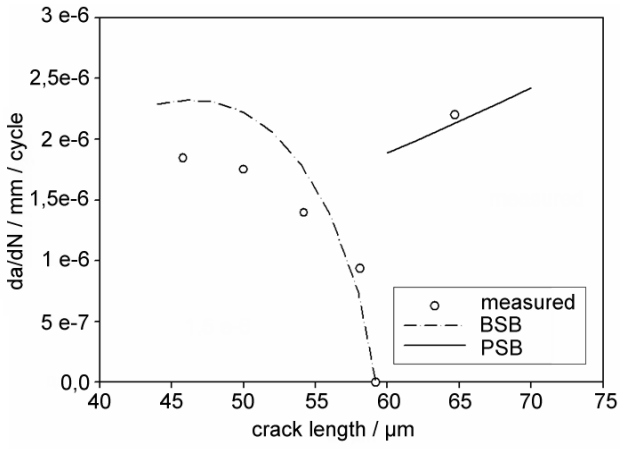

Fig. 3a: Crack growth rate of the cracks initiated at different distances towards the grain boundary

Fig. 3b: Crack propagation rate measured and calculated by the Tanaka-model for a blocked slip band (BSB) and a propagating slip band (PSB)

The observations of the two cracks are in good agreement with the theories based on continuous distributed dislocations [4, 5], which was already applied in literature [20]. With this information the crack propagation rate through the grain boundary was calculated with the Tanaka model quantitatively (Fig. 3b). Thereby, only parameters were used which were measured for single crystals and the grain orientation on both sides of the boundary [21]. The calculation fits the measured crack propagation data quite well for the blocked slip band (BSB) for the stopping crack and with the propagating slip band (PSB) for the growing crack after passing the boundary. But there is no information about the "waiting cycles" which is very important for life time calculation and because there is a great potential for making materials fatigue resistant.

Fatigue crack growth in mild steel: Influence of misorientation angle. Different to the superalloys described above, fatigue crack growth in the mild steel is not dominated by single short cracks overcoming several grain boundaries until one of them leads to failure, but by crack agglomeration of many short cracks which only spread over one or two grains. This behaviour is similar to that observed for martensitic steel reported in literature [22]. The authors discussed the changes in the J-integral due to the presence of neighbouring cracks and the impact of J on the probability of agglomeration. They describe the length distribution and density of short cracks quite well, but still the question remains what causes the strong blocking effect of the grain boundaries. Besides the theoretical models concerning the blocking effect due to dislocation pile up at the grain boundaries, the geometrical aspects of the crack path across a grain boundary are considered in literature [10] as mentioned above. Since a crack has to change its path when overcoming a grain boundary, an area of the grain boundary has to be necessarily fractured to link the crack path on both sides of the boundary. The size of this area rises with increasing angle between the traces of the crack planes on the grain boundary plane. It is assumed that crack propagation is hindered if the angle between the traces is large and in the wake of it the energy for fracturing is too high. In fact, most of the cracks initiated at the micro-notches arrested at the neighbouring grain boundaries.

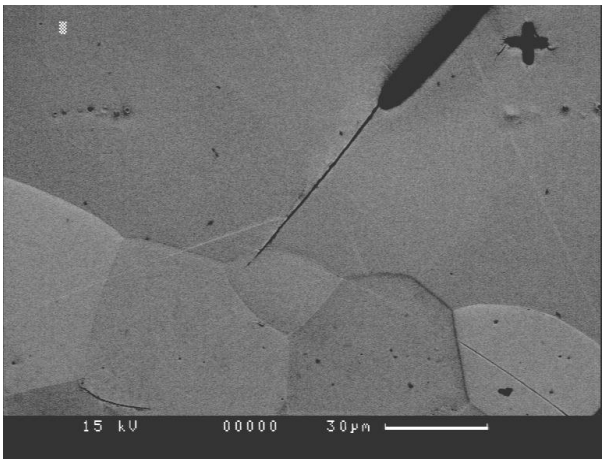

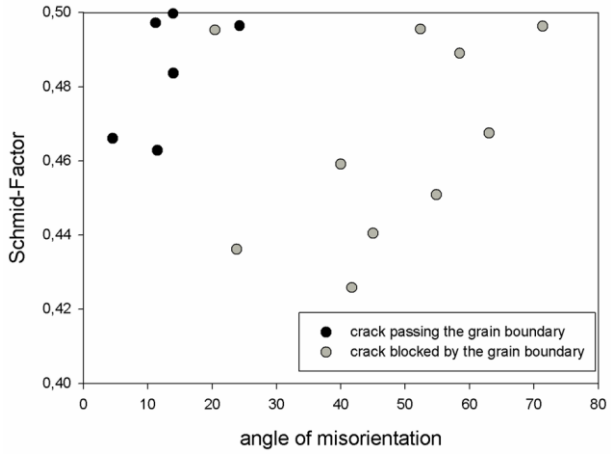

Fig. 4a: Plane stage I crack in steel, obtained by correct orientation of the notches.

Fig. 4b: Blocking effect as function of misorientation and maximum load (Schmid factor)

Only few cracks could overcome the first grain boundary. Figure 10 shows for all investigated cracks the misorientation angle between the crack planes and the pencil glide planes in the neighbouring grains in comparison with the Schmid factor. It can be seen that for all cracks which passed the grain boundary, the misorientation angle was less than 15° and the effective shear stress was high. It can be concluded that the misorientation between neighbouring grains strongly affects the crack advance in the case of the mild steel.

Fatigue crack growth in Al7075-T7: Influence of the grain boundary on the CTOD. In the high strength aluminium alloy all cracks grew perpendicular to the loading axis independently from the crystallographic orientation of the initial grain. In this case a crack initiation on a preferred slip plane was not possible however it was also not necessary. All cracks grew towards the selected high angle grain boundaries. By in-situ measuring the crack opening it is was found that beginning at distance of 6 µm to the boundary the CTOD increase. This increase in the CTOD correlates with a decrease of the crack propagation rate. If the additional crack opening can be used as a measure for the resistance of the boundary against crack propagation is under investigation.

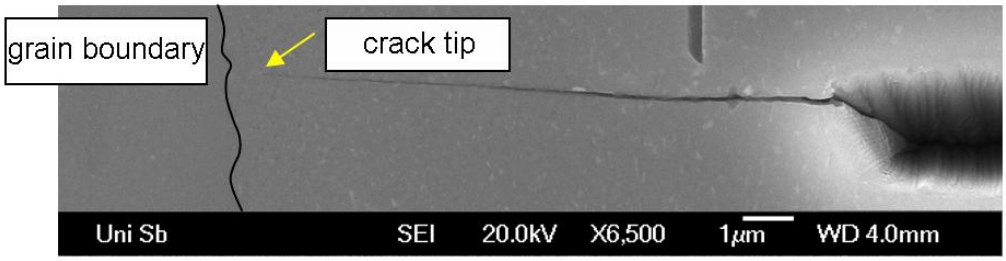

Fig 5a: Crack propagating from a FIB notch (right) towards a grain boundary in Al7075-T7

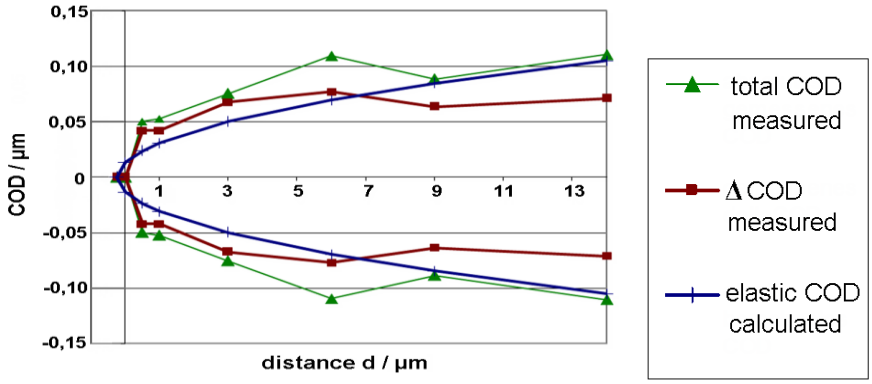

Fig.5b: COD of a crack measured in front of a grain boundary and calculated for an unblocked crack

Fatigue crack growth in bimodal UFG-nickel: Influence of the microstructure. In the case of bimodal UFG-nickel it was found according to literature [23, 24] that the bimodal grain structure leads to a better fatigue resistance. As shown in figure 6a the crack propagation rate is slower at least as long as the crack is short and the threshold for crack propagation is higher than for the coarse grained material as well as for the nanocrystalline as prepared PED-material. This was investigated in situ and figure 6b shows the crack path through a bimodal region. It is obvious that the crack propagates trough the NC part nearly without plasticity while when passing the UFG grains there is a huge plastic deformation visible. It is concluded, that the plasticity of the larger grains leads to the reduced crack propagation while the small NC grains still reveal a good tensile strength of the material. Optimizing this bimodal microstructure by varying the amount of large grains is an on-going work.

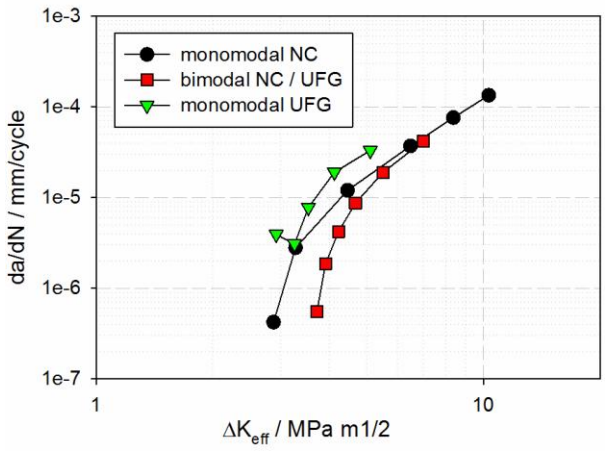

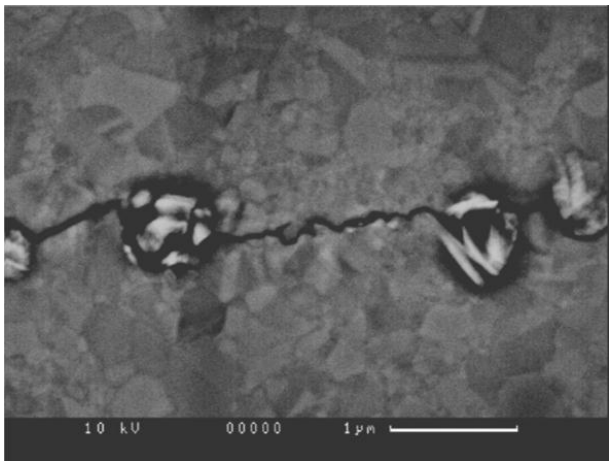

Fig. 6a: Crack propagation rate da/dN as function of ΔK_{eff} for different microstructures

Fig. 6b: Crack path through a NC/ UFG bimodal grain structure with plastic deformed UFG grains

Conclusions

A lot of different influences of microstructural barriers on short fatigue cracks have been investigated systematically by artificial crack initiation with FIB, in-situ investigation in SEM and 3D-FIB tomography. The presented methods are very helpful to understand the interaction mechanisms between fatigue cracks and grain boundaries. The main results are as follows:

- The resistance of a grain boundary in fcc CG-CMSX4 against fatigue crack propagation is determined by the 3D geometry of the active slip planes and systems.
- The total crack length determines the decreasing effect on the crack propagation rate in front of a grain boundary.
- For bcc mild steel there is only a transition of fatigue cracks to neighbouring grains possible for low angle grain boundaries and high loads.
- For Al 7075 T-7 the interaction between crack and grain boundary can be measured and quantified by the CTOD increasing in front of the grain boundary.
- In bimodal NC/UFG nickel the improved crack propagation compared to NC as deposited materials is determined by the plastic deformation behaviour of the UFG grains.

All these mechanisms can now be used to improve materials resistance against crack propagation to make the materials fatigue resistant.

Acknowledgements

The support of this work by the Deutsche Forschungsgemeinschaft (DFG) is gratefully acknowledged.

References:

[1] K.J. Miller, Fatigue Fract. Eng. Mater. Struct., 5, 3 (1982) 223-232
[2] K. Lu, L. Lu, S. Suresh, Science, 324 (2009) 349-352
[3] H. Weiland, J. Nardiello, S. Zaefferer, S. Cheong, J. Papazian, Dierk Raabe, Eng. Fracture Mech., 76, 5 (2009) 709-714
[4] B.A. Bilby, A.H. Cotrell, K.H. Swinden, Proc. R. Soc. London Sect. A, 272 (1963) 304-3
[5] K. Tanaka, Y. Akiniwa, Y. Nakai, R.P. Wei, Eng. Fracture Mech., 24 (1986) 803-819
[6] A. Navarro, E.R. De Los Rios, Phil. Mag. A, 57, 1 (1988) 15-36
[7] Y.H. Zhang, L. Edwards, Scripta Metall. Mater., 26 (1992) 1901-1906
[8] L. Edwards, Y.H. Zhang, Acta Metall. Mater., 42, 4 (1994) 1413-142
[9] L. Edwards, Y.H. Zhang, Acta Metall. Mater., 42, 4 (1994) 1423-1431
[10] T. Zhai, A.J. Wilkinson, J.W. Martin, , Acta Mater., 48 (2000) 4917-4927
[11] T. Zhai, X.P. Jiang, X. J. Li, M.D. Garratt, G.H. Bray, Int. J. Fatigue, 27 (2005) 1202-1209
[12] W. Schaef, M. Marx, H. Vehoff, A. Heckl, P. Randelzhofer, Acta Mater., 59 (2011) 1849-1861
[13] B. Kuenkler, Dueber; P. Koester, U. Krupp; C.P. Fritzen, H.J. Christ, Eng. Fracture Mech. 75, 3-4 (2008) 715-725
[14] E. Ferrie, M. Sauzay, J. of nuclear Mater., 386-88 (2009) 666-669
[15] M. Marx, W. Schaef, H. Vehoff, C. Holzapfel, Mat. Sci. Eng. A, 435/436 (2006) 595-601
[16] C. Holzapfel, W. Schäf, M. Marx, H. Vehoff, F. Mücklich, Scripta Mat., 56 (2007) 697-700
[17] A. Wölffing, diploma thesis, Saarland University (2009)
[18] G.I. Taylor, C.F. Elam, Roy. Proc. Soc. A, 112 (1926) 337
[19] W. Schäf, M. Marx, submitted to Int. J. Fatigue
[20] O. Dueber, B. Kuenkler, U. Krupp, H.J. Christ, C.P. Fritzen, Int. J. Fatigue, 28 (2006) 983-992
[21] W. Schaef, M. Marx, Acta Mater. 60 (2012) 2425–2436
[22] S. Meyer, A. Brückner-Foit, A. Möslang, E. Diegele, Mat.-wiss u. Werkstofftech., 33 (2002) 275-279
[23] H.W. Hoeppel, M. Kautz, C. Xu, M. Murashkin, T.G. Langdon, R.Z. Valiev, H. Mughrabi, Int. J. Fatigue, 28,9 (2006)1001-1010
[24] S. Nelson, L. Ladani, T. Topping, E. Lavernia, Acta Mater., 59 (2011) 3550–3570